

CASCADING OF FAST-MODE BALANCED AND IMBALANCED TURBULENCE

TAKERU K. SUZUKI¹, ALEX LAZARIAN², ANDREY BERESNYAK²

Submitted to ApJ

ABSTRACT

We study the cascading of fast MHD modes in magnetically dominated plasma by performing one-dimensional (1D) dynamical simulations. We find that the cascading becomes more efficient as an angle between wave vector and underlying magnetic field increases and fast mode becomes more compressive. We also consider imbalanced turbulence, in which wave packets propagating in one-direction have more power than those in the opposite direction. Unlike imbalanced Alfvénic turbulence, the imbalanced fast mode turbulence shows faster cascading as the degree of imbalance increases. We found that the spectral index quickly reaches stationary value of -2 . Thus we conclude that the dissipation of fast mode, at least in 1D case, happens not due to weak or strong turbulent cascading, but mostly due to nonlinear steepening.

Subject headings: magnetohydrodynamics – plasma – turbulence

1. INTRODUCTION

Magnetohydrodynamical (MHD) turbulence is ubiquitous in astrophysics. All interstellar medium (ISM) phases are well magnetized with Larmor radius of thermal proton much smaller than outer scale. Molecular clouds are no exception, with compressible, often high-Mach number, magnetic turbulence determining most of their properties (see Elmegreen & Falgarone 1996, Stutzki 2001). Star formation (see McKee & Tan 2002; Elmegreen 2002; Pudritz 2002; Ballesteros-Paredes et al. 2006), cloud chemistry (see Falgarone 1999 and references therein), shattering and coagulation of dust (see Lazarian & Yan 2002 and references therein) are examples of processes for which knowledge of turbulence is absolutely essential. It is also believed that MHD waves and turbulence are important for the acceleration of the solar wind (e.g. Tu & Marsch 1995) as well as winds from stars which possess surface convective layers (e.g. Tsuji 1988).

As MHD turbulence is an extremely complex process, all theoretical constructions should be tested thoroughly. Until very recently matching of observations with theoretical constructions used to be the only way of testing. Indeed, it is very dangerous to do MHD turbulence testing without fully 3D MHD simulations with a distinct inertial range. Theoretical advances related to the anisotropy of MHD turbulence and its scalings (see Shebalin et al. 1983, Higdon 1984, Montgomery, Brawn & Matthaeus 1987, Shebalin & Montgomery 1988, Zank & Matthaeus 1992) were mostly done in relation with the observations of fluctuations in outer heliosphere and solar wind. Computers allowed an important alternative way of dealing with the problem. While still presenting a limited inertial range, they allow to control the input parameters making it easier to test theoretical ideas.

It is well known that linear MHD perturbations can be decomposed into Alfvénic, slow and fast waves with well-

defined dispersion relations (see Alfvén & Fälthammar 1963). The separation into Alfvén and pseudo-Alfvén modes, which are the incompressible limit of Alfvén and slow MHD modes, is an essential element of the Goldreich-Sridhar (1995, henceforth GS95) model of turbulence. There the arguments were provided in favor of Alfvén modes developing a cascade on their own, while the pseudo-Alfvén modes being passively advected by the cascade. The drain of Alfvénic mode energy to pseudo-Alfvén modes was shown to be marginal.

The separation of MHD perturbations into modes in compressible media was discussed further in Lithwick & Goldreich (2001) and Cho & Lazarian (2002, 2003 henceforth CL02, CL03, respectively). Even though MHD turbulence is a highly non-linear phenomenon, the modes does not constitute an entangled inseparable mess.

The actual decomposition of MHD turbulence into Alfvén, slow and fast modes was a challenge that was addressed in CL02, CL03. They studied a particular realization of turbulence with mean magnetic field comparable to the fluctuating magnetic field. This setting is, on one hand, rather typical of the most MHD flows in Galaxy and, on the other hand, allows them to use a statistical procedure of decomposition in the Fourier space, where the bases of the Alfvén, slow and fast perturbations were defined. The entirely different way to decompose modes in high or low- β cases in real space was shown in CL03 was shown to correspond well to this procedure.

In particular, calculations in CL03 demonstrated that fast modes are marginally affected by Alfvén modes and follow acoustic cascade in both high and low β medium. In Yan & Lazarian (2002) and Yan & Lazarian (2004; henceforth YL04) the fast modes were identified as the major agent in scattering of cosmic rays. Similar results in relation to stochastic acceleration of cosmic rays were reached in Cho & Lazarian (2006). Interestingly enough, the dominance of fast modes for both acceleration and scattering is present in spite of the dissipative character of fast modes. The reason for that is isotropy³ of

³ Recent calculations of fast modes interacting with Alfvén modes by Chandran (2005) indicate some anisotropy of fast modes.

¹ School of Arts and Sciences, University of Tokyo, 3-8-1, Komaba, Meguro, Tokyo, 153-8902, Japan

² Department of Astronomy, University of Wisconsin, 475 N. Charter St., Madison, WI 53706
Electronic address: stakeru@providence.c.u-tokyo.ac.jp
Electronic address: lazarian, andrey@astro.wisc.edu

this mode reported in CL03. The Alfvén modes, that are still the default for scattering and acceleration for many researchers, are inefficient due to the elongation of eddies along the magnetic field (Chandran 2000, Yan & Lazarian 2002).

Apart from cosmic rays, acceleration of charged interstellar dust is also dominated by fast modes (Lazarian & Yan 2002, Yan & Lazarian 2003). This provides an additional motivation to studies of properties of fast mode cascade.

The most efficient interaction of fast modes is expected to happen for waves moving in the same direction (see CL02). This indicates that, unlike studies of Alfvén modes for which the 3D character of interactions is essential, the fast modes may be represented by 1D simulations.

In what follows we discuss our code in §2, calculate power spectra in §3, and study cascading of fast modes in §4. We discuss our findings in §5.

2. THE CODE AND THE SIMULATIONS SETUP

We initially give perturbations of fast mode by fluctuations of v_x , v_y , B_y , ρ , and p in magnetically dominated plasma, namely low- β conditions. We dynamically treat time evolution of each variables by solving ideal MHD equations without driving (decay simulation). We do not consider the third (z) component of magnetic field and velocity, which indicates that Alfvén mode is switched off in our simulation, whereas both fast and slow modes are automatically treated. We assume one-dimensional approximation, namely all the physical variables depend only on x ; a wave number vector has only the x -component, namely, $k = k_x$. The number of grid points of the x component is 8192, and the periodic boundary condition is imposed in x -direction.

$$\frac{d\rho}{dt} + \rho \frac{\partial v_x}{\partial x} = 0, \quad (1)$$

$$\rho \frac{dv_x}{dt} = -\frac{\partial p}{\partial x} - \frac{1}{8\pi} \frac{\partial}{\partial x} (B_y^2) \quad (2)$$

$$\rho \frac{d}{dt} (v_y) = \frac{B_x}{4\pi} \frac{\partial B_y}{\partial x}. \quad (3)$$

$$\rho \frac{d}{dt} \left(e + \frac{v^2}{2} + \frac{B^2}{8\pi\rho} \right) + \frac{\partial}{\partial x} \left[\left(p + \frac{B^2}{8\pi} \right) v_x - \frac{B_x}{4\pi} (\mathbf{B} \cdot \mathbf{v}) \right] = 0, \quad (4)$$

$$\frac{\partial B_y}{\partial t} = \frac{\partial}{\partial x} [(v_y B_x - v_x B_y)], \quad (5)$$

where $B^2 = B_x^2 + B_y^2$ and $v^2 = v_x^2 + v_y^2$.

The minimum wave number corresponds to the box size. We set-up $p = 1$, $\rho = 1$, $v_x = 0$, $v_y = 0$ as background conditions. As for directions and strengths of magnetic field, we consider the following four cases: $(B_x, B_y) = (9, 3)$ (strong; quasi-parallel) (3,1) (weak; quasi-perpendicular)

In particular, he shows that contours of isocorrelation for fast modes get oblate with shorter direction along the magnetic field. However, the calculations are performed assuming that Alfvén modes are in the weak turbulence regime. This regime has a limited inertial range. Moreover, anisotropic damping discussed in YL04 is probably a more strong source of anisotropy. Anyhow, the above conclusions about the dominance of fast modes are not altered by the anisotropies that corresponds to squashing contours of isocorrelations in the direction of magnetic field.

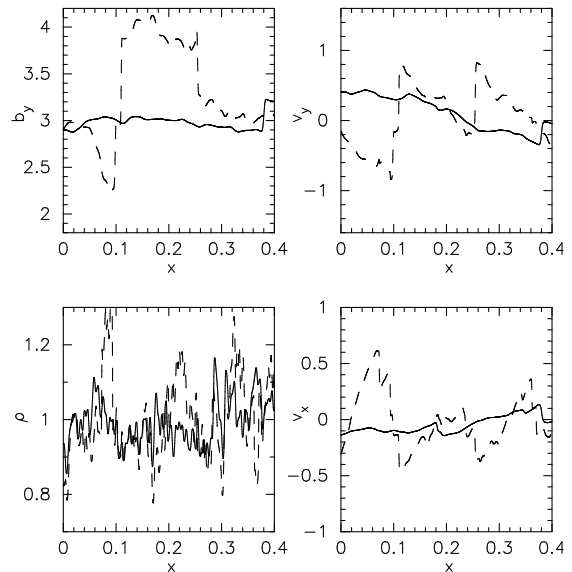


FIG. 1.— Evolution of B_y (upper-left), v_y (upper-right), ρ (lower-left), and v_x (lower-right). Dashed and solid lines are the results at $t = 0.5$ and $t = 3$, respectively.

quasi-parallel), (3,9) (strong; quasi-perpendicular), and (3,1) (weak; quasi-perpendicular). We simulate three cases of a ratio of specific heat, $\gamma = 5/3$ (adiabatic), 1.1, 1.01 (nearly isothermal).

To simulate fast modes we employed 2nd order nonlinear MHD Godunov-MOCCT scheme developed by Sano & Inutsuka 2006 (see also Suzuki & Inutsuka 2005; 2006). In this scheme, each cell boundary is treated as discontinuity, for the time evolution we solve nonlinear Riemann shock tube problems with magnetic pressure by the Rankine-Hugoniot relations. Therefore, entropy generation, namely heating, is automatically calculated from the shock jump condition. A great advantage of our code is that no artificial viscosity is required even for strong MHD shocks; numerical diffusion is suppressed to the minimum level for adopted numerical resolution.

3. TIME EVOLUTION AND POWER SPECTRA

Figure 1 presents time-evolution of reference case ($(B_x, B_y) = (9, 3)$, $\gamma = 1.1$). The initial amplitude is set to be $dB_y = 4.4$, corresponding to super-sonic and sub-Alfvénic condition. Fast modes traveling in both directions have equal energies, we call this balanced turbulence. We tried to reproduce well-known acoustic turbulence solution by setting initial spectral slope to $-3/2$ and random δ -correlated phases for all wavenumbers. The four panels in Figure 1 present B_y , v_y , v_x , and ρ at $t = 0.5$ (dashed) and $t = 3.0$ (solid).

The panels of B_y , v_y , and v_x exhibit many shocks, their strength decreasing in time. In contrast, ρ illustrates more fine scale structure which is actually due to slow mode as we discuss below. Figure 2 shows power spectrum of v , B , and ρ at $t = 0.5$ and 3.0. As expected from Figure 1, v and B exhibit shock dominated spectra, $\propto k^{-2}$. In other words, the acoustic turbulence solution provided initially does not hold for any significant time. The randomness of phases typically assumed in acoustic turbulence or in other theories of weak turbulence breaks down quickly by nonlinear interaction, leading to Burgers-like shock-dominated random state. This is natural, provided that in 1D geometry shocks cannot

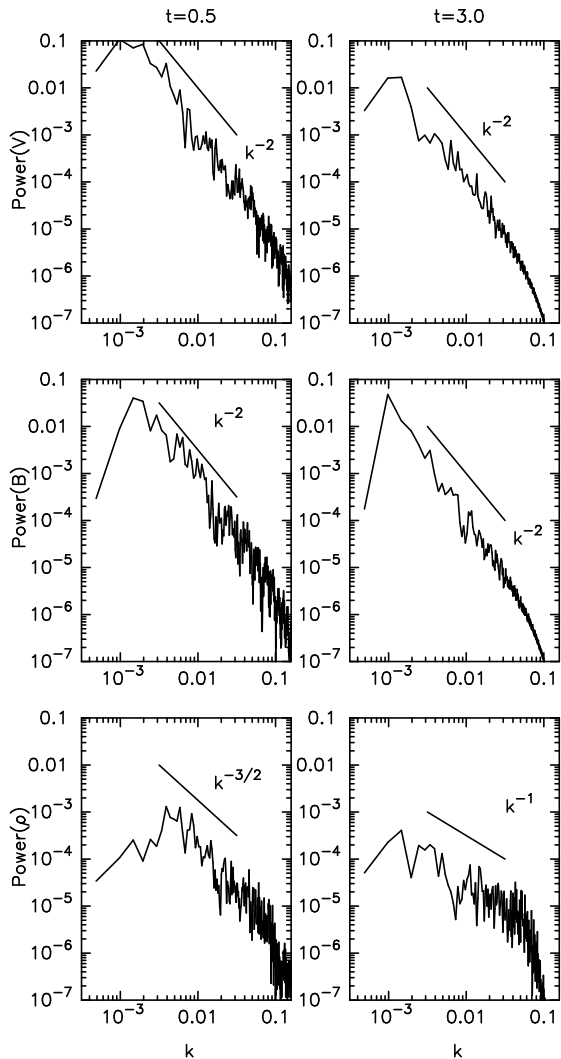


FIG. 2.— Power spectra of v (top), B (middle), and ρ (bottom) at different times, $t = 0.5$ (left) and $t = 3.0$ (right). $k = 1$ corresponds the size of the simulation box.

be diluted geometrically, this increases their relative importance.

Although our initial conditions contain only fast mode, slow mode is generated by nonlinear process of mode interaction. In order to understand the interplay of modes, we decompose all values into fast and slow perturbations (see CL02). Note that this method is statistically correct even for nonlinear waves as discussed in Cho & Lazarian (8).

In Figure 3 we present decomposed spectra of v , B , and ρ at $t = 3.0$. The figure shows that the velocity and magnetic field perturbations are carried by fast mode, while the density perturbations are mostly due to slow mode in accordance with the earlier claims in CL03, Passot & Vázquez-Semadeni (2003) and Beresnyak, Lazarian, & Cho (3). This is because in low- β circumstances the fast wave becomes magnetic mode and the slow wave corresponds to hydrodynamic (acoustic) mode. The amplitude of the slow mode is not as large as that of the fast mode because it is downconverted from the fast mode. The density spectrum of the slow mode which contains small scale structures is shallower than the shock-dominated spectrum of the fast mode. Accordingly, the raw density spectrum (Figure 1) which reflect

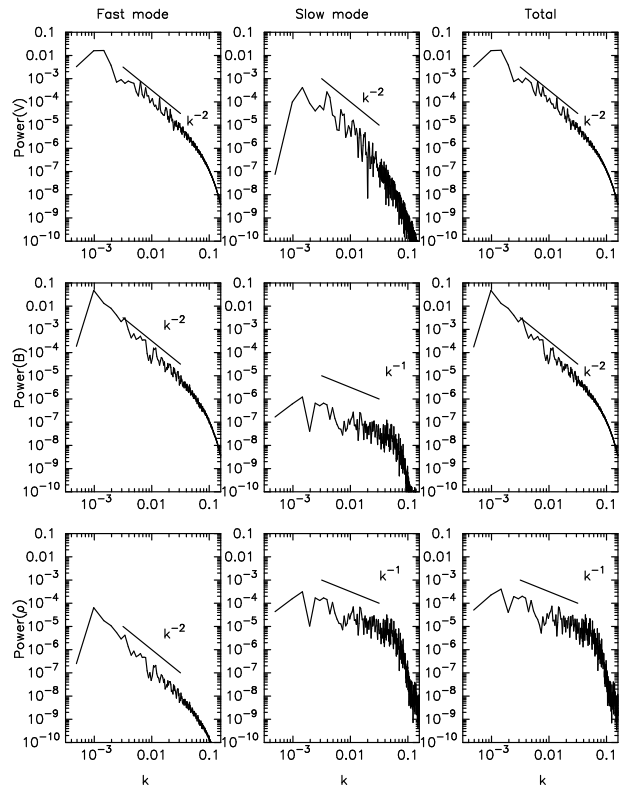


FIG. 3.— Power spectra of v (top), B (middle), and ρ (bottom) decomposed into fast (left) and slow (middle) modes at $t = 3.0$. Composed values are shown on the right for comparison.

the slow mode is also shallower than the spectra of v and B . Unlike fast modes, however, we expect the slow modes evolve very differently in 1D and 3D. Therefore here we concentrate on the evolution of the fast mode only.

4. CASCADING OF FAST MODE

From now on we analyze evolution of integrated energy density (energy column density), $\int dx(\rho\delta v^2 + \delta B^2)/2$, of the decaying fast modes.

4.1. Dependence on Initial Amplitude

Figure 4 shows dissipation of fast mode energy as a function of time for different initial amplitudes with the same background $(B_x, B_y) = (9, 3)$. The figure indicates that larger amplitude gives faster damping. This is reasonable since the dissipation is owing to nonlinear processes such as shocks and wave-wave interactions. Damping times, which are defined as slopes of the respective lines, becomes longer at later times as the amplitudes decrease, which is also consistent with the nonlinear dissipation through steepening.

4.2. quasi-Parallel vs. quasi-Perpendicular

Figure 5 compares the energy of the fast modes of quasi-parallel ($B_x = 9, B_y = 3$) and quasi-perpendicular ($B_x = 3, B_y = 9$) cases. The same $dB_y = 4.4$ and $\gamma = 1.1$ are adopted. The figure shows that the dissipation is more effective in the quasi-perpendicular case. This is because the fast mode shows more compressive character as an angle between the propagation and the magnetic field increases and the shock dissipation is enhanced (Suzuki, Yan, Lazarian, & Cassinelli 2006).

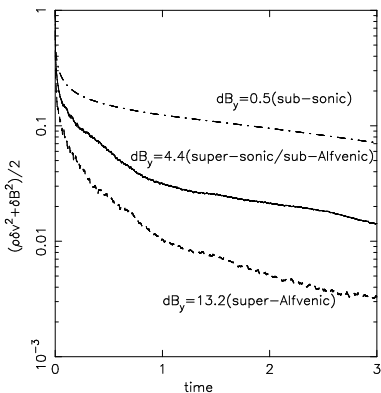


FIG. 4.— Energy of the fast modes of various initial amplitudes. The background field strength is $(B_x, B_y) = (9, 3)$. Dot-dashed, solid, and dashed lines are results of $dB_y = 0.5$ (sub-sonic), 4.4 (super-sonic/sub-Alfvénic), and 13.2 (super-Alfvénic). The initial energy density is normalized at unity in each case.

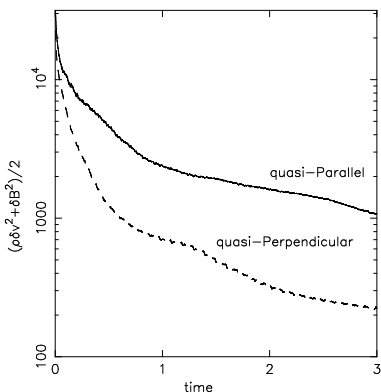


FIG. 5.— Energy of the fast modes of the quasi-parallel, $(B_x, B_y) = (9, 3)$, (solid) and quasi-perpendicular, $(B_x, B_y) = (3, 9)$, (dashed) cases.

4.3. Dependence on Plasma- β

Dependence on plasma- β is very weak provided the plasma is kept magnetically dominated ($\beta < 0.5$) during simulations. However, if β approaches unity, the dissipation becomes saturated. Figure 6 compares cases with the same $(B_x, B_y) = (9, 3)$ (left) or $(B_x, B_y) = (3, 9)$ (right) and $dB_y = 13.2$ but different $\gamma = 1.1$ (dotted) and $5/3$ (solid). In the case with $\gamma = 5/3$ the plasma is heated up so that the gas pressure eventually becomes comparable with the magnetic pressure ($\beta \simeq 1$). In contrast, the plasma β stays well below unity in the cases with $\gamma = 1.1$ because the heating is less efficient due to the smaller γ . Figure 6 shows that once the plasma- β becomes unity the dissipation is suppressed in the case with $\gamma = 5/3$, while the energy density monotonically decreases in the case with $\gamma = 1.1$.

At later epochs in the case with $\gamma = 5/3$, slow mode also has a sizable amount of energy because the phase speed of the slow mode becomes comparable with that of the fast mode. This tendency is more extreme in the quasi-perpendicular case (the right panel), because the plasma is heated up more due to larger compressibility.

4.4. Balanced vs. Imbalanced

Figure 7 compares the evolution of fast modes in balanced and fully-imbalanced cases. The background field strength is $(B_x, B_y) = (9, 3)$. Dot-dashed line indicates total fast mode energy in balanced case with $dB_y = 4.4$,

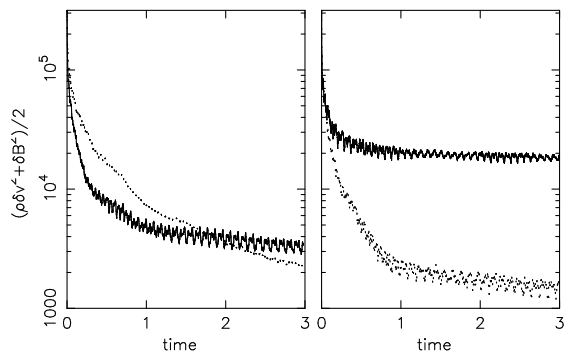


FIG. 6.— *left* : Energy of the fast modes of different $\gamma = 1.1$ (dotted) and $5/3$ (solid). The same background field strength, $(B_x, B_y) = (9, 3)$, and amplitude, dB_y , are adopted. *right* : the same as the left panel but for $(B_x, B_y) = (3, 9)$.

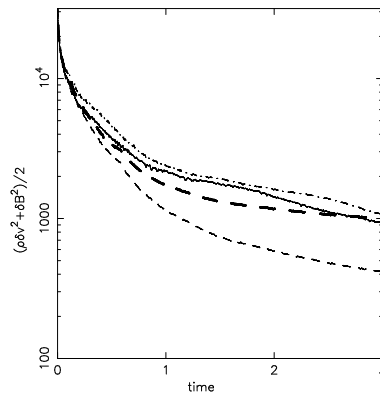


FIG. 7.— Comparison of balanced and imbalanced fast mode turbulence. Dot-dashed line indicates total fast mode energy in balanced case with $dB_y = 4.4$, solid line indicates fast mode energy propagating to one direction in balanced case with $dB_y = 6.2$, and dashed line denotes fast mode energy in imbalanced case with $dB_y = 4.4$. Thick dashed line is the same case which includes the bulk kinetic energy in addition to the turbulent energy.

solid line indicates fast mode energy propagating to one direction in balanced case with $dB_y = 6.2$, and dashed line denotes fast mode energy in imbalanced case with $dB_y = 4.4$. Note that the energy is proportional to dB_y^2 so that the initial values of these three lines are the same. The figure shows that the imbalanced cascade is more dissipative, which is opposed to the tendency obtained in the Alfvénic turbulences.

One reason is different nature of the dissipation of fast and Alfvén modes. The fast mode is isotropic. The dissipation occurs among fast waves which meet the following resonance conditions (see CL02):

$$\omega_1 + \omega_2 = \omega_3, \quad (6)$$

$$\mathbf{k}_1 + \mathbf{k}_2 = \mathbf{k}_3. \quad (7)$$

Since, $\omega \propto k$ for the fast modes, the resonance conditions can be satisfied only when all three \mathbf{k} vectors are collinear. When parent '1' and '2' waves propagate in the counter directions, (difference signs of \mathbf{k}_1 and \mathbf{k}_2) the daughter wave should have smaller wavenumber, \mathbf{k}_3 , (larger wavelength).

In contrast, if parent waves propagate in the same direction, wavenumber of the daughter wave becomes larger than the parents', which is more appropriate for the dissipation. In the imbalanced case, we only have fast modes traveling in the same direction so that the

resonances selectively generate waves with shorter wavelengths which suffer faster dissipation. Dot-dashed (energy of one direction in balanced case with $dB_y = 6.2$) and dashed (imbalanced case with $dB_y = 4.4$) lines show very similar damping at the beginning. This indicates that the dissipation of 1D fast mode turbulence is controlled by wave packets traveling in the same direction and almost independent of those in the counter directions, since the initial energy of one direction in the former case is identical to the initial total energy of the latter.

The second reason why the imbalanced fast mode turbulence is different from Alfvén one is bulk acceleration. In order to study the effect of the motion of the system, we also plot the sum of the fast mode energy and the kinetic energy of the bulk motion in the imbalanced case (thick dashed line). The attenuation of this combined energies is quite similar to the results of the balance case with the same amplitude in one direction ($dB_y = 6.2$). The imbalanced flux of fast mode transfers the momentum to the fluid. As a result, the system is accelerated into the direction corresponding to the initial wave momentum flux. Generally, energy density of waves is lost in accelerating fluid by transfer of the momentum flux to the gas even though the waves themselves do not suffer damping (14). This might also account for the faster dissipation of the fast mode energy density in the imbalanced turbulence.

5. DISCUSSIONS

Our study has confirmed the cascading of fast modes happens due to the interaction of modes moving in the same direction as it was discussed earlier (see CL02). However, we have obtained spectrum of fast modes that is close to -2 , rather than to the acoustic turbulence spectrum $-3/2$ suggested in CL02. The difference may be due to the difference of 1D vs. 3D cases. It is clear that further research into this difference is necessary.

We have also found that as the amplitude of compressions increase, the non-linear damping of turbulence speeds up. In our adiabatic calculations the restoring force was increasing due to medium heating and as the result the non-linear steepening and cascading slowed down. Similarly, for the modes that compress both magnetic field and gas, the rate of dissipation was less compared to the modes that mostly compress the gas.

We find that the imbalanced fast modes dissipate in a different way than Alfvén ones. For the Alfvén turbulence cascading is due to wave packets moving in the opposite direction, therefore, the imbalance makes the cascading less efficient. For fast modes waves moving in the same direction interact more efficiently. We confirmed that the oppositely moving fast modes are not essential for the cascading.

Cascading of imbalanced fast modes is important for the problem of streaming instability evolution, which is the part of the picture of both galactic leaky box model

⁴ It is easy to see that if the injection happens at scale L with Alfvén Mach number $M_A = V/V_A$, where V_A is the Alfvén velocity that arises from the total magnetic field in the fluid, the range for weak turbulence is limited by $[L, LM_A^2]$. While the regime of weak

and the acceleration of particles in shocks. This instability arises from the flow of particles along the magnetic field direction and reflects the particles back (Kulsrud & Pearce 1968). Our results indicate that the fast modes cascading limits the instability even in the absence of both damping and the ambient turbulence (YL02, Farmer & Goldreich 2004).

Turbulence may be very different in 1D and 3D. We find, however, that our attempts to get insight into the dynamics of fast modes using 1D model is meaningful, as the possible transversal deviation δk is limited. Assuming that the fast modes follow the acoustic cascade with the cascading time

$$\tau_k = \omega/k^2 v_k^2 = (k/L)^{-1/2} \times V_{ph}/V^2, \quad (8)$$

YL04 used the uncertainty condition $\delta\omega t_{cas} \sim 1$, where $\delta\omega \sim V_{ph}\delta k(\delta k/k)$ to estimate δk

$$\delta k/k \simeq \frac{1}{(kL)^{1/4}} \left(\frac{V}{V_{ph}} \right)^{1/2}. \quad (9)$$

Eq. (9) provides a very rough estimate of how much the randomization of vectors is expected due to the fast mode cascading. This estimates suggests that down the cascade for $kL \gg 1$ the approximation of waves moving in the same direction could be accurate enough.

In this paper we dealt with fast modes irrespectively of the evolution of the other modes. This possibility corresponds to the earlier theoretical and numerical studies (GS95, Lithwick & Goldreich 2001, CL02, CL03). Recently, however, Chandran (2005) discussed the interaction between fast and Alfvén modes under the approximation that the latter constitute *weak* turbulence, i.e. turbulence that cascades slowly due to weak non-linearities. We expect appreciable mitigation of the Alfvén-fast mode interaction compared to those in Chandran (2005), when Alfvénic turbulence is *strong*, i.e. when the turbulence evolves fast, over just one wave period. We feel that the resulting large disparity in the rate of evolution of the Alfvénic and fast modes should result in much less cascading of fast modes by the Alfvénic modes compared to the case of the weak Alfvénic turbulence. Note, that strong Alfvénic turbulence is default for most astrophysical situations, while the inertial range of the weak Alfvénic turbulence is limited⁴ Goldreich & Sridhar 1997, Lazarian & Vishniac 1999). In our next paper we shall provide calculations of the fast modes interaction with the Alfvénic modes.

Acknowledgments

T.K.S. was supported by JSPS Research Fellow for Young Scientist, 4607, during carrying out this research. AL acknowledges the support of the NSF Center for Magnetic Self-Organization in Laboratory and Astrophysical Plasmas and the NSF grant AST-0307869 and NSF-ATM-0312282. AB acknowledges the support of the Ice Cube project.

Alfvénic turbulence can still be important (see Lazarian 2006), in most astrophysical situations that regime of strong Alfvénic turbulence covers much longer inertial range.

REFERENCES

Alfvén, H. & Fälthammar, C.-G. 1964, *Zeitschrift für Astrophysik*, 58, 292

Ballesteros-Paredes, J., Klessen, R. S., MacLow M.-M., & Vázquez-Semadeni, E. 2006, *Proto-Stars & Planets V*, pre-print (astro-ph/0603357)

- Beresnyak, A., Lazarian, A., Cho, J. 2005, *ApJ*, 624, L93
Chandran, B. D. G. 2000, *Phys. Rev. Lett.*, 85, 4656
Chandran, B. D. G. 2005, *Phys. Rev. Lett.*, 95, 5004
Cho, J., Lazarian, A., & Vishniac, E. T. 2003, *Turbulence and magnetic fields in astrophysics*, eds. T. Passot & E. Falgarone, LNP 614, Springer, Berlin, astro-ph/0205286
Cho, J. & Lazarian, A. (2002), *Phys. Rev. Lett.*, 88, 245001
Cho, J. & Lazarian, A. (2003), *MNRAS*, 345, 325 - 339
Elmegreen, B. C. & Falgarone, E. 1996, *ApJ*, 471, 816
Elmegreen, B. C. 2002, *ApJ*, 577, 206
Farmer, A. J. & Goldreich, P. 2004, 604, 671
Goldreich, P. & Sridhar, S. 1995, *ApJ*, 438, 763
Goldreich, P. & Sridhar, S. 1997, *ApJ*, 485, 680
Higdon, J. C. 1984, *ApJ*, 285, 109
Jacques, S. A. 1977, *ApJ*, 215, 942
Kim, J. & Ryu, D. 2005, *ApJ*, 630, L45
Kulsrud & Pearce 1968
Lazarian, A. 2006, *ApJL*, 645, L25
Lazarian, A. & Vishniac, E. 1999, *ApJ*, 517, 700
Lazarian, A. & Yan, H. 2002, *ApJ*, 556, L105
Lithwick, Y. & Goldreich, P. 2001, *ApJ*, 562, 279
McKee, C. F. & Tan, J. C. 2002, *Nature*, 6876, 59
Montgomery, D., Brawn, M. R., & Matthaeus, W. H. 1987, *J. Geophys. Res.*, 92, 282
Passot T. & Vázquez-Semadeni, E. 2003, *A&A*, 398, 845
Pudritz, R. E. 2002, *Science*, 295, 68
hebalin, J. V., Matthaeus, W. H., & Montgomery, D. 1983, *J. Plasma Phys.*, 29, 525
Shebalin, J. V. & Montgomery, D. 1988, *J. Plasma, Phys.*, 39, 339
Stutzki, J. 2001, *Ap&SSSupp.*, 277, 39
Suzuki, T. K., Yan, H., Lazarian, A., Cassinelli, J. P. 2006, *ApJ*, in press
Suzuki, T. K. & Inutsuka, S. 2005, *ApJ*, 632, L49
Suzuki, T. K. & Inutsuka, S. 2006, *J. Geophys. Res.*, in press
Tsuji, T. 1988, *A&A*, 197, 185
Tu, C.-Y. & Marsch, E. 1995, *Space Sci. Rev.*, 73, 1
Yan, H. & Lazarian, A. 2002, *Phys. Rev. Lett.*, 89, 1102
Yan, H. & Lazarian, A. 2003, *ApJ*, 592, L33
Yan, H. & Lazarian, A. 2004, *ApJ*, 614, 757
Zank, G. P. & Matthaeus, W. H. 1992, *J. Geophys. Res.*, 97, 17189